Combustion, Explosion, and Shock Waves, Vol. 48, No. 5, pp. 625–635, 2012.

Influence of Aluminum Particle Size on Ignition and Nonstationary Combustion of Heterogeneous Condensed Systems

V. A. Arkhipov[a,b], S. S. Bondarchuk[a,b], A. G. Korotkikh[c], V. T. Kuznetsov[a], A. A. Gromov[c], S. A. Volkov[d], and L. N. Revyagin[d]

UDC 629.194.632.1:536.46

Translated from *Fizika Goreniya i Vzryva*, Vol. 48, No. 5, pp. 148–159, September–October, 2012.
Original article submitted December 2, 2011; revision submitted January 18, 2012.

Abstract: The results of studies of the effect of particle size of aluminum powder in condensed systems on the ignition, nonstationary combustion, and acoustic conductivity of the burning surface are presented. Analysis of the experimental data shows that the ignition delay and the temperature of burning surface of the heterogeneous condensed systems under study decrease with increasing particle size of aluminum powder, and the nature of the dependence of the nonstationary burning rate on the time of depressurization of the combustion chamber for compositions containing micron or ultrafine aluminum powders is in qualitative agreement with the phenomenological theory of nonstationary combustion. Replacement of micron aluminum powder by ultrafine powder in a heterogeneous condensed system increases acoustic conductivity.

Keywords: heterogeneous condensed systems, aluminum powder, aluminum particle size, conductive ignition, radiant flux, nonstationary combustion, acoustic conductivity.

DOI: 10.1134/S0010508212050140

INTRODUCTION

One of the promising directions in developing a new generation of heterogeneous condensed systems (HCS) is the replacement of aluminum powders of micron size (e.g., the ASD industrial powders) by ultrafine powders, whose particles are orders of magnitude smaller in size. The first experimental studies on the use of aluminum in HCS were performed in the USSR (Institute of Chemical Physics, USSR Academy of Sciences) in the 1960s–1970s under the direction of Leipunskii [1] and Gen [2]. Aluminum particles were prepared by evaporation and condensation of aluminum vapors in argon. The size of the forming particles was varied by changing the evaporation and condensation modes. We obtained encouraging results in terms of improving the energy characteristics of HCS due to more complete combustion of aluminum and reduction of the size of aluminum particles in the combustion products. These studies were performed in the laboratory using small HCS samples. Further, the studies were suspended for several reasons, primarily because of lack of technologies to produce large quantities of ultrafine powder of aluminum with chemically stable particles and because of lack of information on the combustion physics and agglomeration of nanoparticles in HCS.

The research on the use of ultrafine powder in HCS [3–5] was activated in the late 1990s and is being continued to the present time. That is due to the following factors.

[a] Scientific Research Institute of Applied Mathematics and Mechanics of Tomsk State University, Tomsk, 634050 Russia; leva@niipmm.tsu.ru.
[b] Institute of Problems of Chemical and Energetic Technologies, Siberian Branch, Russian Academy of Sciences, Biisk, 659322 Russia.
[c] Tomsk Polytechnic University, Tomsk, 634050 Russia; korotkikh@tpu.ru.
[d] Tomsk State University, Tomsk, 634050 Russia.

— Traditional HCS compositions containing micron aluminum powders 3–20 μm in diameter have completely exhausted their potential opportunities, and no fundamentally new results to improve their energy performance are expected soon.

— The progress in the technology of obtaining ultrafine powder (in particular, by electric explosion of wires [6]) allows one to produce sufficiently large quantities of ultrafine metal powders with controlled properties, size distribution of particles, and high stability.

— Studies [7–12] have shown that the use of ultrafine aluminum powder in HCS is promising not only in terms of increasing energy characteristics, but also in terms of reducing the agglomeration on the burning surface of samples, increasing the burning rate, and controlling the exponent in the burning rate law.

Analysis of the results of studies of stationary combustion of HCS containing ultrafine aluminum powders is given in review articles [13, 14] and monographs [15]. In this paper, we present the results of studies of nonstationary effects in conductive and radiative ignition, combustion with rapid depressurization and quenching in the combustion chamber, and the results of studies of the acoustic conductivity of the burning surface that characterizes the susceptibility of heterogeneous condensed systems to oscillatory combustion.

ULTRAFINE ALUMINUM POWDER

The powder particle size is one of the most important characteristics of the systems under consideration, which determines their properties and behavior in ignition, combustion, and quenching. Due to the intensive development of powder nanotechnologies, multiphase flow mechanics, and diagnostic methods, the problems of adequately describing the size spectrum of polydisperse systems, identifying experimentally obtained size distributions of particles (usually, histograms), and approximating them by a suitable probability density function are becoming relevant.

Analysis of the published data on the particle-size distribution of different polydisperse systems showed that almost all metal powders with unimodal (one-vertex) distribution functions can be described by a generalized gamma or log-normal distribution.

Arkhipov et al. [16] considered an identification algorithm for unimodal size distributions of aluminum powder particles using experimental histograms based on the formulation and solution of the inverse problem and finding an extremum of the corresponding functional by direct search. The approach was tested by studying the ASD-4 (Fig. 1a), ASD-6, and ASD-8 micron aluminum powders widely used in modern HCS compositions and the Alex ultrafine aluminum powder (Fig. 1b) produced by electric explosion of wires in argon. Mass and number distribution functions of particles of the powders under study are shown in Table 1. The average diameters of the powders were calculated on the basis of number distributions. It was found that the mass average diameter of the Alex ultrafine aluminum powder particles is 12–40 times smaller than that of the ASD micron powders. In storage, the Alex powder particles aggregate and form "grape bunches" (Fig. 1b) due to the electric charge accumulated on the particle surface and the greater surface energy. The source of the aggregation of small particles is large particles of ultrafine aluminum powder of diameter 0.3–0.6 μm.

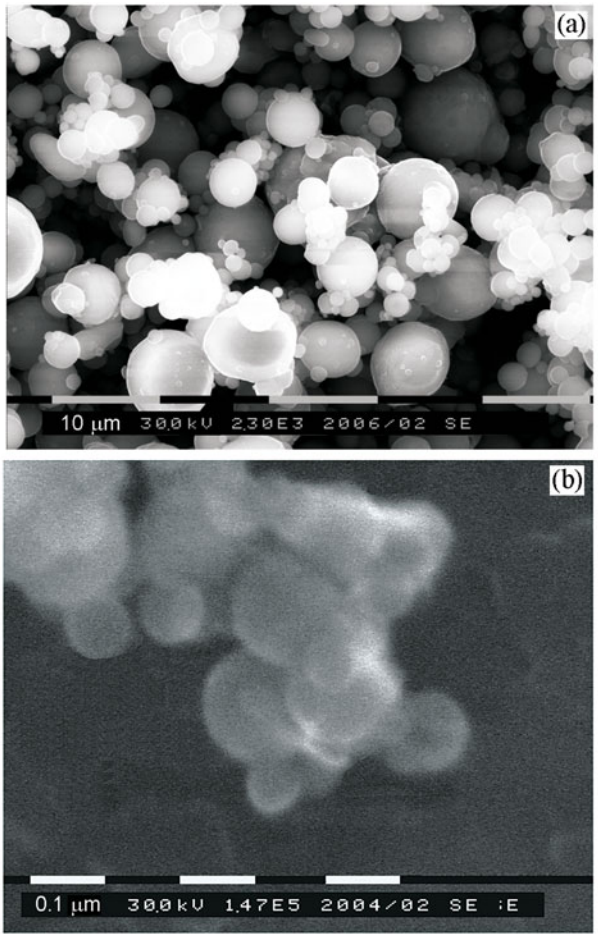

Fig. 1. Photomicrograph of ASD-4 micron aluminum powder (a) and Alex ultrafine aluminum powder (b).

Table 1. Average statistical diameters and distribution functions of aluminum powders

Powder	d_{10}, μm	d_{20}, μm	d_{30}, μm	d_{32}, μm	d_{43}, μm	Distribution function, μm^{-1}
ASD-4	1.23	1.66	2.28	4.34	7.34	$g(d) = 0.064d^{1.21}\exp(-0.303d)$
ASD-6	0.85	1.17	1.60	3.01	4.72	$g(d) = 0.147d^{1.64}\exp(-0.561d)$
ASD-8	0.72	0.90	1.09	1.60	2.11	$g(d) = 2.29d^{3.15}\exp(-1.97d)$
Alex	0.12	0.13	0.14	0.16	0.18	$f(d) = 28.7 \cdot 10^6 d^{4.49}\exp(-46.8d)$

Note: d_{10}, d_{20}, d_{30}, d_{32}, and d_{43} are average number, RMS, volume average, volume–surface average, and mass average diameters; $g(d)$ and $f(d)$ are the mass and number distribution functions.

Table 2. Activity parameters of aluminum powders

Powder brand	T_{ox}, °C	α, % (660°C)	α, % (1000°C)	v_{ox}, mg/s (at T, °C)	C_{Al}, %	δ, nm	ρ_b, g/cm^3
ASD-4	820	2.5	41.8	0.05 (970–980)	98.7	10.8	1.06
Alex	548	39.4	45.0	0.05 (541–554)	86.0	3.1	0.15

Note: T_{ox} is the intense oxidation temperature, α is the degree of oxidation, v_{ox} is the maximum oxidation rate, C_{Al} is the mass aluminum content, δ is the calculated thickness of the Al_2O_3 oxide layer, and ρ_b is the bulk density of the powder.

Transition from compact to ultrafine state changes the thermodynamic properties of the metal powders, shifting the equilibrium lines of chemical reactions and phase transformations. Upon reaching threshold temperatures of 200–500°C the reactivity increases many times. Increased chemical activity, small thickness, and oxide shell structure facilitate the sintering of nanosized metal particles. Thus, the ultrafine nickel and copper powders obtained by an electrical explosion in argon are sintered at temperatures of ≈145 and 100°C, and the ultrafine aluminum powders, even at room temperature [6, 17, 18].

The activity parameters of aluminum powders from data of differential thermal analysis are presented in Table 2 [15] . As the particle size of aluminum powder increases, the metal content and bulk density of the powder decrease. The rapid oxidation temperature of the ASD-4 (660°C) micron powder is much higher than the melting point of aluminum, and it is even lower for the Alex ultrafine powder being equal to 548°C. The degree of oxidation of the ASD-4 micron aluminum powder does not exceed 2.5%, and it is 39.4% for the ultrafine powder when heated to the melting point. The maximum oxidation rate for both types of aluminum powders is the same, but is reached in different temperature ranges: 970–980°C for ASD-4 and 541–554°C for Alex. The oxide layer thickness was calculated by the formula

$$\delta = \frac{d_{43}}{2}\left\{1 - \left[1 + \left(\frac{1}{z_{Al}} - 1\right)\frac{\rho_{Al}}{\rho_{Al_2O_3}}\right]^{-1/3}\right\},$$

where z_{Al} and ρ_{Al} are the mass fraction and density of aluminum and $\rho_{Al_2O_3}$ is the density of aluminum oxide. The oxide layer thickness of the ultrafine aluminum particles determined by this formula with an average size $d_{32} = 0.18$ μm is 3.5 times smaller than that of the ASD-4 micron powder. According to data of electron microscopy studies [18], the oxide layer of the Alex ultrafine powder particles obtained by an electrical explosion in argon has a loose structure and its thickness is ≈2.5 nm.

Ultrafine powders have a low bulk density and are hardly pressed (e.g., the bulk density of the Alex ultrafine aluminum powder is lower than that of the ASD-4 micron powder). The large specific surface area of the Alex ultrafine powder increases the content of adsorbed impurities.

METHODS OF THE STUDY

Ignition of HCS

The ignition of HCS under radiant heating was studied using an Uran-1 setup (Fig. 2a) and a CO_2 continuous laser (Fig. 2b) [19, 20]. The ignition delay time t_{ign} of HCS samples in the experiments was determined by the appearance of a visible flame recorded by a photodiode or an ionization detector. The HCS samples were cylinders 10 mm in diameter and 5 mm in height. The studies were performed in air under normal conditions, i.e., in a medium containing an oxidizer

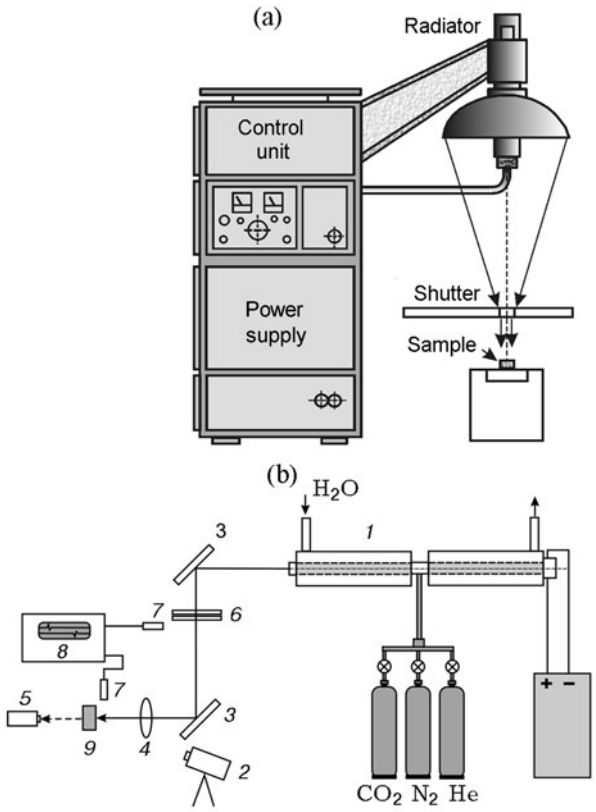

Fig. 2. Diagram of the setups for integral radiative heating of HCS (Uran-1) (a) and monochromatic (CO_2 laser) radiative heating of HCS (b): (*1*) optical maser; (*2*) Jade J 530 SB thermal imaging camera; (*3*) gold sputtered mirror; (*4*) sodium chloride lens; (*5*) driving head of the IMO-2 average output power meter; (*6*) electromechanical shutter; (*7*) photodiode; (*8*) OWON digital oscilloscope; (*9*) HCS sample under study.

(oxygen). The effect of the ovidizer concentration in the surrounding gaseous medium on the characteristics of the HCS ignition was considered in several works. In particular, it has been shown [21, 22] that with considerable intensity of heat fluxes (above a certain threshold), the mechanism of ignition of non-metal HCS and ballistite powders transforms from solid-phase ignition to the gas-phase model. For semivolatile HCS, the solid-phase thermal ignition theory was shown to adequately describe the initial stage of combustion [23].

The integrated radiant flux (in a broad range of wavelengths) from the DKsR-10000 xenon lamp of Uran-1 (Fig. 2a) was focused by an elliptical mirror into a spot 12 mm in diameter. The distribution of the radiation in the spectral ranges was as follows: 0.5 kW (9%) in the ultraviolet part of the spectrum, 2 kW (36%) in the visible range, and 3 kW (55%) in the infrared range. The radiation intensity of the Uran-1 setup was measured by a calorimetric method with a relative accuracy of 10%. We used disc-shaped copper calorimeters 10 mm in diameter and 3 mm in thickness. The surface of the disc which absorbed the radiation was covered with lamp black. On the non-blackened surface of the disc, a thermocouple was mounted at a depth of 1.5 mm. We measured the rate of temperature changes of the copper disc under the influence of the radiation coming to the blackened surface of the disc, and calculated the radiant heat flux by the formula

$$q = \frac{mc}{(1-R)S}\frac{\Delta T}{\Delta t},$$

where m is the mass of the disc, c is the specific heat, R is the reflectance, S is the blackened area of the disc surface, and $\Delta T/\Delta t$ is the rate of temperature changes.

The ionization detector electrodes were placed at a distance of 3–5 mm from the HCS sample. When exposed to light, the output electrical signal from the FD-9K photodiode triggered an ChZ-54 electronic counting frequency meter. The appearance of a flame activated the ionization detector, whose signal was also fed to the frequency counter. The ignition delay time of the HCS was determined from the frequency counter readings.

The ignition of HCS by a monochromatic heat flux was studied on a setup based on a CO_2 continuous laser with a wavelength of 10.6 μm and a maximum power of 100 W (Fig. 2b). The ignition delay time of the HCS was determined by the signals of two photodiodes, one of which triggered a digital storage oscilloscope by opening the shutter and the other recorded the appearance of the visible flame of the sample. The power of the laser incident on the HCS sample was measured by an IMO-2 average output power meter. Simultaneously, the ignition surface temperature fields of the studied HCS compositions was recorded with a Jade J 530 SB thermal imager with digital recording on a PC in the infrared spectral range (2.5–2.7 μm) at a frequency of 100 Hz. The relative error in measuring the temperature by the thermal imager was 5%.

The HCS ignition by a heated body was studied under conductive heating on a hot metal plate (Fig. 3) in the temperature range 320–480°C. The plate surface temperature was measured with a thermocouple. Its junction was pressed into a channel drilled on the back side of the plate at a distance of 1 mm from the external (working) surface of the plate directly in the contact area with the surface of the ignited sample. The thermocouple EMF was measured by a microvoltmeter. The thermocouple was calibrated against a mercury thermometer in the temperature range 0–600°C with an accuracy not more than ±1°C. The HCS sample under

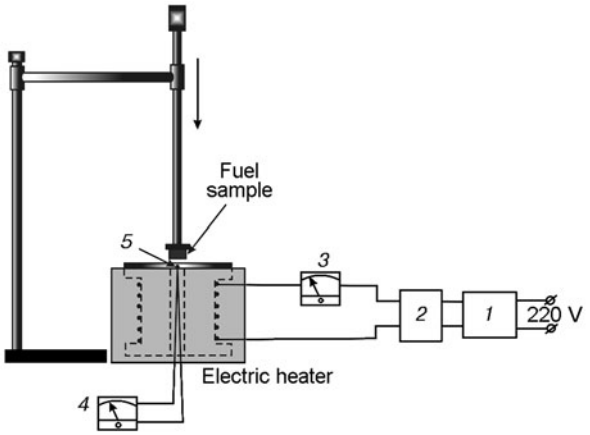

Fig. 3. Diagram of the conductive heating of the HCS: (*1*) voltage stabilizer; (*2*) autotransformer; (*3*) ammeter; (*4*) microvoltmeter; (*5*) thermocouple.

study was attached to a holder which freely moved in the vertical direction along a guide rod. To exclude the thermal influence of the holder, its material was chosen have thermophysical characteristics close to the corresponding HCS characteristics (asbestos cement composition). The HCS sample was pressed to a heated metal plate with a force of ≈3 N. The moment of ignition of the HCS was determined by the appearance of flame. The ignition delay t_{ign} was taken to be the time from the moment of contact of the sample with the heated plate until the appearance of visible flame.

To obtain each value of the ignition delay of the HCS composition under study, we performed 3-5 duplicate tests. The relative measurement error (which characterizes the scatter of experimental data) at a confidence level of 0.95 was 8–18%.

Nonstationary Combustion Processes of the HCS

A review paper [24] presents two independent methods of measuring the nonstationary burning rate without causing disturbances in the combustion of the HCS: high-speed shooting of the burning surface and the method of inverse problems of internal ballistics based on recording the dependence of pressure on time during the transition process of rapid depressurization of a semi-enclosed volume.

The combustion of the HCS with rapid depressurization of a semi-enclosed volume selected for the analysis of the considered methods of measuring transient velocity is of undoubted practical interest (cut-off of the propulsion system thrust, quenching of propellant, etc.), and also plays an important role in testing physicomathematical models of nonstationary combustion of condensed systems [25, 26]. Some versions of this method use the hypothesis of quasistationary discharge with the opening of additional nozzles for depressurization and subsequent propellant quenching. Arkhipov et al. [24] proposed a method of measuring nonstationary burning rate based on nonstationary discharge during the transition process.

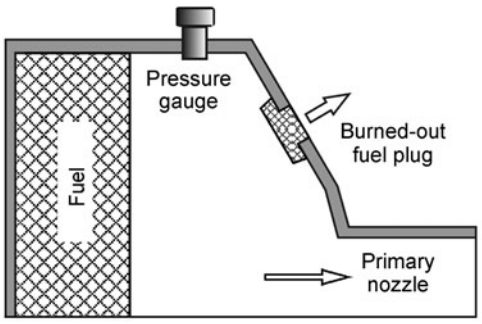

Fig. 4. Diagram of the combustion chamber with an additional nozzle.

The measurements in [24] were performed in a model solid propellant with a cylindrical combustion chamber 50 mm in diameter and 100 mm in length with two nozzles (primary nozzle and secondary nozzle) (Fig. 4). To ensure the adiabatic process, the internal walls of the combustion chamber were insulated by inserts of a material with low thermal conductivity (textolite inserts). The primary nozzle diameter was calculated for the main regime of stationary combustion of the sample at a pressure of p_0 ≈4.0 MPa. The secondary nozzle diameter was varied to change the depressurization rate. The secondary nozzle was tightly covered with a burned-out plug of ballistite gunpowder in the shape of a mushroom.

After ignition of the HCS sample, the combustion in the chamber became stationary (p_0 = const) due to combustion of the sample and the powder tube. The burn-out and discharge of the plug were followed by rapid depressurization in the combustion chamber, whose depth dp/dt was determined by the free volume of the chamber and the ratio of the critical section diameters of the primary and secondary nozzles.

The pressure curve $p(t)$ recorded during the transition process was used to determine the nonstationary burning rate $u(t)$ by solving the inverse problem of internal ballistics [24].

Study of Acoustic Conductivity of the Burning Surface of the HCS

The standard way to measure the acoustic conductivity of the burning surface of HCS is to use a T-chamber, which has simultaneously flammable disc-

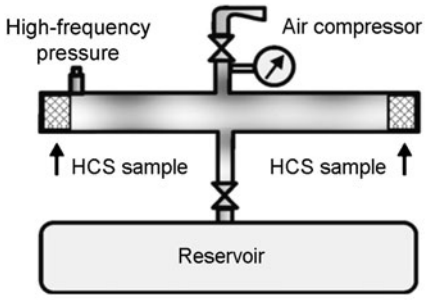

Fig. 5. Diagram of the setup for measuring the acoustic conductivity of the HCS (T-chamber).

shaped samples of HCS at the opposite ends [27]. The experimental setup is shown schematically in Fig. 5. It includes a combustion chamber (T-chamber) 42 mm in inner diameter, HCS samples under study, a reservoir 80 dm^3 in volume, and a compressed air supply system. A piezoelectric sensor was placed in the chamber to measure pressure fluctuations, and a test gauge was used to measure the average pressure level. The setup design allows the average chamber pressure to be varied in the range 1.5–10 MPa, the frequency of pressure fluctuations in the range 0.5–4 kHz (due to changes in the length of the T-chamber), the initial temperature of the HCS samples in the range −30 to 50°C, and the burning surface area of the samples (due to the presence of longitudinal gaps on their end surfaces.)

The HCS sample height was selected in the range 10–14 mm in order to choose a parameter value $n = S_{sp}/S_{ch}$ (S_{sp} is the burning surface area of the sample and S_{ch} is the surface area of the chamber end) produces only the first harmonic of longitudinal oscillations.

RESULTS OF THE STUDY

Ignition Delay Time of the HCS

In the experiments, we determined the ignition delay of the HCS under study, containing aluminum powder of different particle sizes, for various radiation densities and temperatures of the heated block (Figs. 6–7).

The influence of the aluminum powder particle size on the ignition by CO_2laser was studied for two basic HCS (Table 3). The oxidizer excess coefficient of both compositions was 0.55. We used the ASD-4 and Alex aluminum powders as metal fuel. The particle size of ammonium nitrate, HMX, and ammonium perchlorate ranged within 160–315 μm. Cylindrical HCS samples 10 mm in diameter and 30 mm in height were prepared by mechanical mixing of the initial components, followed by through or dull pressing at a pressure of ≈215 MPa and vulcanization. The density of the cured samples was ρ_{sp} = 1.4–1.65 g/cm^3 depending on the component ratio. In duplicate experiments for the same composition, the variation in the density of the samples was not greater than 0.02 g/cm^3 The porosity of the samples was considered insignificant and was not controlled. The sample surface to be irradiated was produced immediately before the experiment by cutting by a microtome knife. The sample height was 5 mm. Its end surface was smooth, with no depressions and protrusions. The end surface of the HCS compositions was covered by lamp black to reduce the optical inhomogeneity.

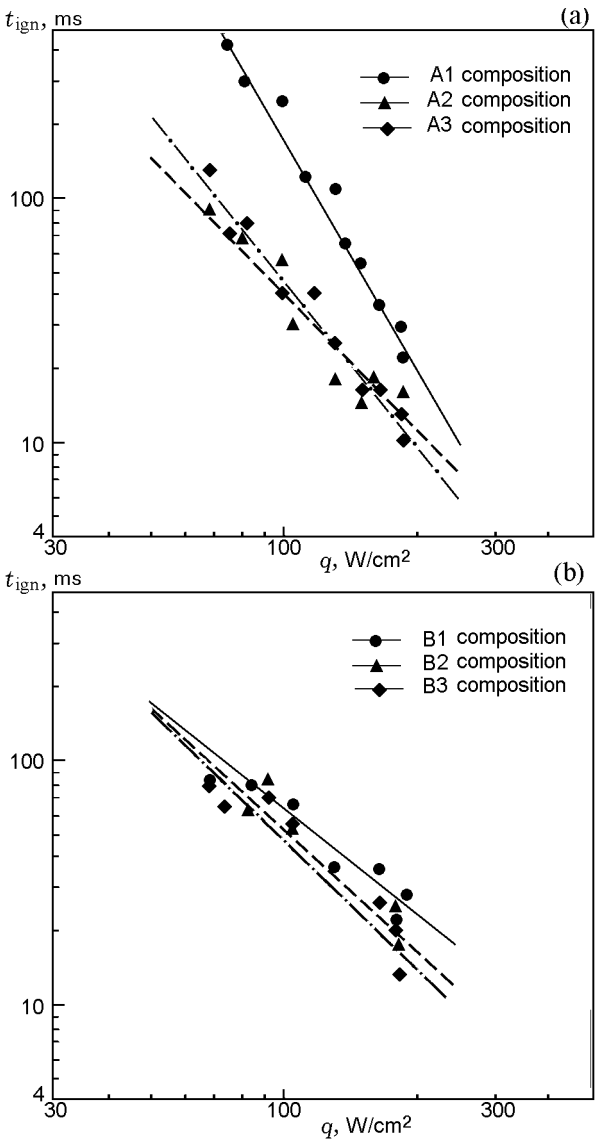

Fig. 6. Ignition delay of various HCS compositions (see Table 3) versus radiation flux density (CO_2 laser).

Table 3. Compositions of the HCS under study (CO_2 laser)

Composition	Mass content of the components, %						
	AN	HMX	AP	MPVT-LD	SKDM-80	Alex	ASD-4
A1	28	28	—	24	—	—	20
A2	28	28	—	24	—	10	10
A3	28	28	—	24	—	20	—
B1	29	29	15	—	12	—	15
B2	29	29	15	—	12	5	10
B3	29	29	15	—	12	15	—

Note: AN is ammonium nitrate, AP is ammonium perchlorate, MPVT-LD is a tetrazole copolymer plasticized by mixed nitroester plasticizer, and SKDM-80 is butadiene rubber plasticized by transformer oil.

It is found that lamp black on the burning surface of samples does not affect the chemical decomposition of the components during laser ignition of HCS. Analysis of the results (see Fig. 6) showed that with increasing radiant flux density, the influence of addition of the Alex ultrafine aluminum powder decreases for the studied composition A based on ammonium nitrate, HMX, and active fuel binder. In the range of radiant heat flux densities of 70–130 W/cm^2, the ignition delay of the composition A3 containing Alex ultrafine powder is 4.5–6.0 times smaller than that of A1, which includes the ASD-4 micron powder. With higher heat flux density, the influence of the dispersed aluminum powder decreases. The efficiency ratio is the ratio of the ignition delay of the HCS containing micron aluminum powder to the ignition delay time of the HCS containing ultrafine powder. For the basic composition B, it is insignificant (K = 1.0–2.1) compared to the basic composition A. Apparently, this is due to the thermal resistance of the fuel binder used, an increase in the temperature in the reaction layer of the condensed phase, and the increased role of heterogeneous reactions in the HCS ignition. Increasing the aluminum powder particle size in the HCS decreases the ignition delay, the amount of supplied heat, and the reaction layer thickness of the HCS. Due to the low temperature of rapid oxidation (see Table 2) and high chemical activity, the Alex ultrafine powder increases the heat flux to the condensed phase and, accordingly, increases the rate of the chemical reactions in the condensed layer of the HCS. The results of thermal analysis of the HCS composition A2 showed that the maximum rate of the chemical reactions is in the temperature range 220–230°C and rapid oxidation begins at 224°C. In the temperature range 550–582°C the Alex ultrafine powder additive makes an additional contribution to the process of heat release.

Table 4. Compositions of the HCS under study (Uran-1)

Composition	Mass content of components, %				
	AP	BR	HTPB	Alex	ASD-4
1	72	18	—	—	10
2	72	18	—	10	—
3	62	—	18	—	20
4	62	—	18	20	—

Note: BR is butyl rubber and HTPB is hydroxyl-terminated polybutadiene rubber.

Thermal imaging of ignition [28] of the basic HCS composition A with constant emissivity of the sample surface ε = 0.95 showed that, at a radiant heat flux density of 60 W/cm^2, the appearance of visible flame of the compositions A2 and A3 containing Alex occurs near the condensed phase of the sample surface at moderate temperatures of 660 and 545°C. For the composition A1 containing ASD-4, visible flame appears at an average surface temperature of ≈715°C, accomanied by melting and foaming of the fuel binder. With further supply of heat, the outflow of gaseous decomposition products of the oxidizer and fuel binder slows down. It is assumed that due to large aluminum particles, the reaction layer thickness increases and heat release due to chemical reactions occurs in deep layers.

At a certain temperature, the gaseous products of decomposition of the oxidizer and fuel binder are rapidly released with discharge of the condensed layer of the sample into the flame zone. The dispersed layer burns with intense heat release. The average surface temperature of the sample increases sharply to 820°C, the ASD-4 aluminum powder reacts, and a self-sustaining combustion regime of the HCS is established.

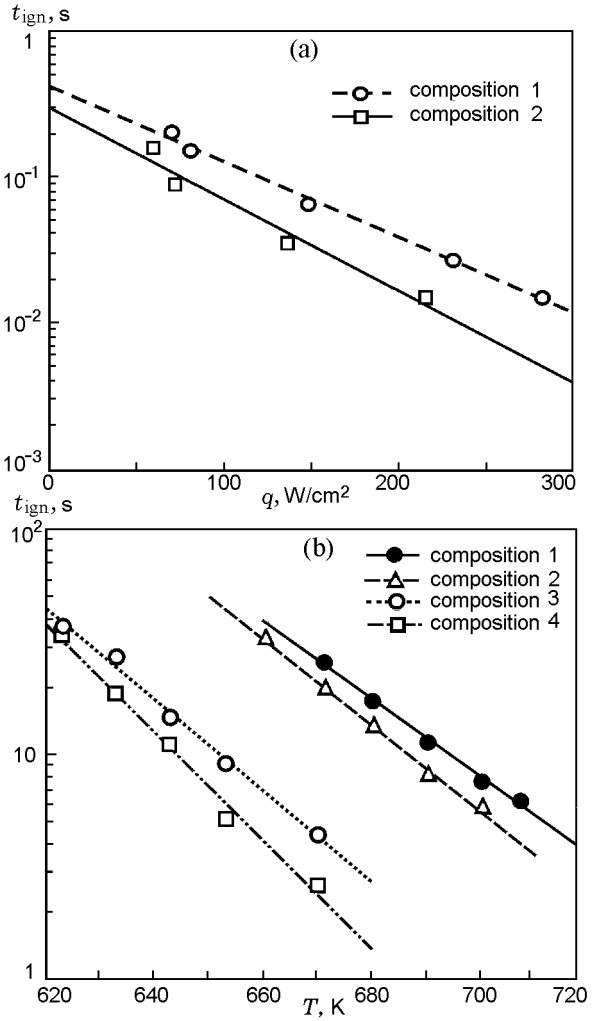

Fig. 7. Ignition delay of various HCS compositions (see Table 4) versus radiation flux density (Uran-1) (a) and the temperature of the heated block (conductive heating) (b).

The Uran-1 integral radiant heating and conductive heating setups were used to study the model compositions of the HCS under study (Table 4) based on AP and inert fuel-binder (butyl rubber and hydroxyl-terminated polybutadiene rubber) with the addition of aluminum powder.

Analysis of the results (see Fig. 7a) showed that the ignition delay of composition 1 containing ASD-4 decreases from 0.20 to 0.015 s with increasing heat flux density in the range of 70–280 W/cm^2 and for composition 2 containing Alex it decreases from 0.16 to 0.015 s in the radiant flux density range of 58–214 W/cm^2. With the same radiant flux density, the ignition delay of the HCS containing Alex is smaller than that of the compositions with ASD-4, and the difference increases with increasing flux density.

The conductive heating setup was used to measure the ignition delay of the HCS with variation in the surface temperature of the heated block (see Fig. 7b). The data in the figure show that with increasing surface temperature of the block, the efficiency ratio of the Alex ultrafine aluminum powder increases.

The influence of ultrafine aluminum powder on the ignition of the HCS is determined by the possibility of rapid oxidation of aluminum powder particles on the burning surface or in the immediate vicinity of it. If oxidation of aluminum particles occurs in the heated layer, an abnormal ignition regime is possible. Such a regime was found in the ignition of HCS with ultrafine aluminum powder with heat supply from a heated block [19, 29], when the flame appearance was accompanied by a loud sound effect, surface layer cracking, its fragmentation, and burnout. When heating by integral luminous heat flux, anomalous ignition of the HCS was observed only when a metal plate was on the sample surface.

Nonstationary Burning Rate of the HCS

The effect of the aluminum powder particle size on the burning rate during depressurization of the combustion chamber was studied using a model HCS composition containing 41% AP, 30% HMX, 14% SKDM-80, and 15% aluminum powder (Alex or ASD-4) of varying particle size [30, 31]. We used samples 40 mm in diameter and 30 mm in height reinforced on the lateral surface. Preliminarily, we measured the stationary burning rate of the model HCS composition in a bomb of constant volume at an ambient pressure of 0.1–6.0 MPa and determined the pressure dependence of the burning rate: $u = 1.14p^{0.4}$ for the composition with ASD-4 and $u = 1.35p^{0.47}$ for the composition with Alex (u in mm/s and p in atm).

Figure 8 presents the results of study of the nonstationary burning rate of the model HCS containing ASD-4 or Alex. The dependence $u(t)$ calculated on the basis of Zel'dovich phenomenological theory [26] (surface temperature $T_s = \text{const}$), agrees qualitatively with the measured dependence, with a quantitative discrepancy of up to 32% for the composition with ASD-4.

Analysis of the results obtained for the nonstationary burning rate of the HCS (see Fig. 8) showed that during the transient combustion, the dependence $u(t)$ for the composition with ASD-4 is oscillatory with a frequency of about 4 Hz. In this case, the deviation of $u(t)$ from quasistationary combustion can reach 32%. For the composition with Alex, the dependence $u(t)$ is also oscillatory with about the same frequency, though the deviation from the quasistationary value is less—28%.

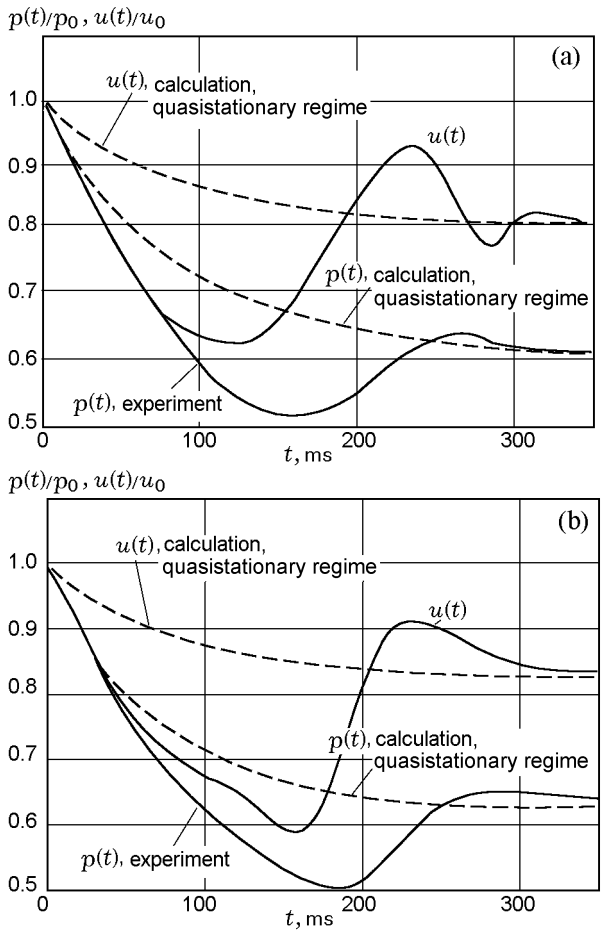

Fig. 8. Burning rate of the HCS composition based on AP, HMX, and SKDM-80 containing Alex powder (a) and ASD-4 powder (b) versus time of opening of the secondary nozzle.

Acoustic Conductivity of the Burning Surface of the HCS

The effect of the particle size and the content of aluminum powders on the acoustic conductivity of the burning surface was studied using a model HCS composition based on AP and SKDM-80 butyl rubber containing up to 17.5% (by weight) aluminum powder. In the T-chamber, a series of experiments was performed to study the acoustic conductivity of the model HCS composition. Analysis of the results (Fig. 9) showed that the pressure increase in the combustion chamber leads to reduction of the maximum acoustic conductivity and to a shift of this maximum to the range of high frequencies. That is, an increase in combustion chamber pressure impairs the wave amplification on the burning surface of the HCS. A significant effect on the acoustic conductivity of the model composition is exerted by the mass content and particle size of the aluminum powder.

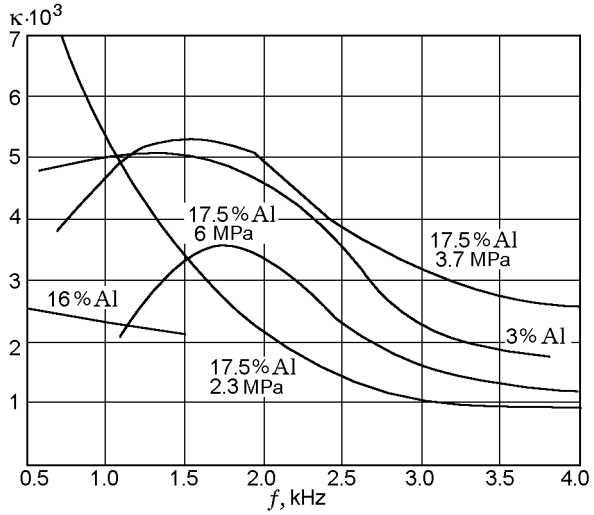

Fig. 9. Acoustic conductivity of the HCS composition based on AP and SKDM-80 versus frequency with different content of ASD-4 and pressure variation in the T-chamber.

Increasing the mass content of the ASD-4 powder in the HCS from 3 to 16% stabilizes combustion due to damping of acoustic vibrations by aluminum oxide particles which are condensed combustion products. Replacing the ASD-4 micron aluminum powder by the Alex ultrafine powder increases the acoustic conductivity of the burning surface of the sample and reduces the damping in the volume of the T-chamber [27].

CONCLUSIONS

1. The ignition delay of the heterogeneous condensed systems decreases with increasing particle size of the aluminum powder due to small particle size and small oxide layer thickness, lower temperature of the beginning of rapid oxidation, and the high chemical activity of the Alex ultrafine aluminum powder, which increases the rate of heat transfer into the condensed reaction layer.

2. The appearance of visible flame of the HCS based on ammonium nitrate and energy fuel binder containing the Alex ultrafine aluminum powder, at a heat flux density of 60 W/cm^2 occurs near the surface of the condensed phase of the sample at an average temperature of ≈545°C. Decreasing the aluminum powder particle size in the HCS increases the average ignition surface temperature, heating time, and reaction layer thickness and decreases the rate of chemical reactions.

3. Experiments with rapid depressurization of the combustion chamber showed the stabilizing influence of the ultrafine aluminum powder (compared to the mi-

cron size powder) on the combustion of the heterogeneous condensed system. The amplitude of the burning rate oscillation with respect to the quasistationary dependence $u(t)$ for the studied composition with Alex ultrafine aluminum powder is smaller than that for the composition with micron aluminum powder. This indicates that the introduction of ultrafine powder reduces the dependence of the nonstationary burning rate of the HCS on the pressure change rate in the combustion chamber.

4. The acoustic conductivity of the heterogeneous condensed systems is significantly affected by the mass content and particle size of aluminum powder. Increasing the content of the ASD-4 micron aluminum powder in the fuel from 3 to 16% stabilizes the combustion process, which is associated with the damping of acoustic vibrations by the condensed combustion products—aluminum oxide particles. Replacement of micron aluminum powder by ultrafine powder increases the acoustic conductivity of the burning surface of the sample and reduces the damping in the volume of the T-chamber, thus increasing the possibility of oscillatory combustion in the combustion chamber.

The work was performed as part of the federal target program "Research and Development in Priority Areas of Development of the Scientific-Technological Complex of Russia for 2007–2013 Years" on the subject "Application of Metal Nanopowders in Energy and Ceramic Technologies" (State Contract No. 2011-1.9-519-001-020).

REFERENCES

1. A. A. Zenin, A. P. Glazkova, O. I. Leipunskii, and V. K. Bobolev, "Effect of Aluminum on the Burning of Ammonium Perchloratepolyformaldehyde Mixtures," Fiz. Goreniya Vzryva **4** (3), 299–304 (1968) [Combust., Expl., Shock Waves **4** (3), 165–168 (1968)].
2. M. Ya. Gen, Yu. V. Frolov, and V. B. Storozhev, "Combustion of Submicron Aluminum Particles," Fiz. Goreniya Vzryva, **14** (5), 153–155 (1978) [Combust., Expl., Shock Waves **14** (5), 675–676 (1978)].
3. M. M. Mench, C. L. Yen, and K. K. Kuo, "Propellant Burning Rate Enhancement and Thermal Behavior of Ultra-Fine Aluminum Powders (Alex)," in *Energetic Materials: Production, Processing and Characterization, 29th Int. Annu. Conf. of ICT, Karlsruhe, Germany, 30-1–30-15, 1998.*
4. V. N. Simonenko and V. E. Zarko, "Comparative Studying the Combustion Behavior of Fine Aluminum," in *Energetic Materials: Production, Processing and Characterization, 30th Int. Annu. Conf. of ICT, Karlsruhe, Germany, 21-1–21-14, 1999.*
5. L. T. DeLuca, F. Cozzi, S. Manenti, et al., "Ballistic Testing of Clean Solid Rocket Propellants," in *Energetic Materials: Production, Processing and Characterization, 32nd Int. Annu. Conf. of ICT, Karlsruhe, Germany, 10-1–10-14, 2001.*
6. M. I. Lerner, "Electroexplosive Nanopowders of Inorganic Materials: Production Technology, Features, Applications," Doct. Dissertation of Engineering Science (Tomsk, 2007).
7. M. M. Mench, K. K. Kuo, C. L. Yeb, and Y. C. Lu, "Comparison of Thermal Behavior of Regular and Ultrafine Aluminum Powders (Alex) Made from Plasma Explosion Process," Combust. Sci. Technol. **135**, 269–292 (1998).
8. E. W. Price, "Combustion of Metallized Propellants," *Fundamentals of Solid-Propellant Combustion*, in *Progress in Astronautic and Aeronautic*, Vol. 90, Ed. by K. K. Kuo and M. Summerfield (1994), pp. 479–513.
9. A. I. Atwood, K. P. Ford, D. T. Bui, P. O. Curran, and T. Lyle, "Radiant Ignition Studies of Ammonium Perchlorate Based Propellants," Progress in Propulsion Physics, Ed. by L. DeLuca, C. Bonnal, O. Haidn, and S. Frolov, Vol. 1 (Torus Press, Moscow, 2009), pp. 121–140.
10. V. A. Arkhipov, A. G. Korotkikh, V. T. Kuznetsov, and L. A. Savel'eva, "Influence of Particle size of Metal Additives on the Burning Rate of Mixed Compositions," Khim. Fiz. **23** (9), 18–21 (2004).
11. O. G. Glotov, D. A. Yagodnikov, V. S. Vorob'ev, V. E. Zarko, and V. N. Simonenko, "Ignition, Combustion, and Agglomeration of Encapsulated Aluminum Particles in a Composite Solid Propellant. II. Experimental Studies of Agglomeration," Fiz. Goreniya Vzryva **43** (3), 83–97 (2007) [Combust., Expl., Shock Waves **14** (5), 320–333 (2007)].
12. Yu. V. Frolov, A. N. Pivkin, and D. A. Ivanov, "The Particle Structure and Combustion Parameters of Nanoaluminum Compositions," Khim. Fiz. **27** (6), 54–61 (2008).
13. L. T. De Luca, L. Galfetti, F. Severini, et al., "Burning of Nano-Aluminized Composite Rocket Propellants," Fiz. Goreniya Vzryva **41** (6), 80–94 (2005) [Combust., Expl., Shock Waves **41** (6), 680–692 (2005)].
14. G. V. Sakovich, V. A. Arkhipov, A. B. Vorozhtsov, S. S. Bondarchuk, and B. V. Pevchenko, "The Study of Combustion of HEMs with Aluminum Nanopowders," Ross. Nanotekhnol. **5** (1–2), 89–101 (2010).
15. *Combustion of Metal Nanopowders*, Eds. by A. A. Gromov, V. A. Arkhipov, A. G. Korotkikh, et al. (Del'taplan, Tomsk, 2008) [in Russian].
16. V. A. Arkhipov, S. S. Bondarchuk, A. G. Korotkikh, M. I. Lerner, "Burning of Nano-Aluminized Composite Rocket Propellants," Gorn. Zh., No. 4, 58–65 (2006).

17. V. V. Danilenko, *Synthesis and Sintering of Diamonds by Explosions* (Energoatomizdat, Moscow, 2003) [in Russian].
18. A. P. Il'in and A. A. Gromov, *Combustion of Aluminum and Boron in a Hyperfine State* (Izd. Tomsk. Univ., Tomsk, 2002) [in Russian].
19. V. A. Arkhipov, A. G. Korotkikh, V. T. Kuznetsov, and E. S. Sinogina, "Influence of Dispersed Metal Powders on the Characteristics of Conductive and Radiative Ignition of Mixed Compositions," Khim. Fiz. **26** (6), 58–67 (2007).
20. V. A. Arkhipov, A. G. Korotkikh, V. T. Kuznetsov, A. A. Razdobrev, and I. A. Evseenko, "The influence of particle size on the performance of aluminum powder Ignition mixed compositions laser," Khim. Fiz. **30** (7), 68–76 (2011).
21. V. N. Simonenko, V. E. Zarko, and A. B. Kiskin, *Study of Nonstationary Combustion Regimes of Ballistite Powders*, Preprint No. 10 (Inst. of Chem. Kinet. and Combust., Sib. Branch, Russian Acad. of Sci., 1980).
22. V. T. Kuznetsov, V. P. Marusin and A. I. Skorik, "Ignition Mechanism in a Heterogeneous System," Fiz. Goreniya Vzryva, **10** (4), 526–529 (1974) [Combust., Expl., Shock Waves **10** (4), 680–692 (1974)].
23. I. G. Assovskii, *Combustion and Internal Ballistics* (Nauka, Moscow, 2005) [in Russian].
24. V. A. Arkhipov, S. S. Bondarchuk and A. G. Korotkikh, "Comparative Analysis of Methods for Measuring the Transient Burning Rate. I. Research Methods," Fiz. Goreniya Vzryva **46** (5), 82–87 (2010) [Combust., Expl., Shock Waves **46** (5), 564–569 (2010)].
25. B. V. Novozhilov, *Nonstationary Burning of Solid Propellants* (Nauka, Moscow, 1973) [in Russian].
26. Ya. B. Zel'dovich, O. I. Leipunskii, and V. B. Librovich, *The Theory of Nonstationary Gunpowder Combustion* (Nauka, Moscow, 1975).
27. V. A. Arkhipov, S. A. Volkov, and L. N. Revyagin, "Experimental Study of the Acoustic Admittance of the Burning Surface of Composite Solid Propellants," Fiz. Goreniya Vzryva **47** (2), 74–80 (2011) [Combust., Expl., Shock Waves **47** (2), 193–199 (2011)].
28. V. A. Arkhipov and A. G. Korotkikh, "The Influence of Aluminum Powder Dispersity on Composite Solid Propellants Ignitability by Laser Radiation," Combust. Flame **159**, 409–415 (2012).
29. V. A. Arkhipov, A. G. Korotkikh, and V. T. Kuznetsov, "Ignition and Combustion of Composite Solid Propellants Containing Ultrafine Metal Powders," Izv. Ross. Akad. Raket. Art. Nauk, **1** (42), 18–25 (2005).
30. V. A. Arkhipov, S. S. Bondarchuk, and A. G. Korotkikh, "Comparative Analysis of Methods for Measuring the Transient Burning Rate. I. Research Methods," Fiz. Goreniya Vzryva **46** (5), 88–96 (2010) [Combust., Expl., Shock Waves **46** (5), 564–569 (2010)].
31. V. A. Arkhipov, S. S. Bondarchuk, A. G. Korotkikh, A. B. Vorozhtsov, A. Bandera, L. Galfeti, L. De Luca, and G. Colombo, "Nonstationary Effects in Combustion of High-Energy Nanocomposites," Izv. Vyssh. Uchebn. Zaved., Fiz. **50** (9/2), 3–12 (2007).